The *Nf2* tumor suppressor regulates cell–cell adhesion during tissue fusion

Margaret E. McLaughlin*†, Genevieve M. Kruger*, Kelly L. Slocum*‡, Denise Crowley*‡, Norman A. Michaud§, Jennifer Huang*, Margaret Magendantz*, and Tyler Jacks*‡¶

*Department of Biology and Center for Cancer Research, Massachusetts Institute of Technology, Cambridge, MA 02139; †Department of Pathology, Brigham and Women's Hospital, Boston, MA 02115; ‡Howard Hughes Medical Institute, Chevy Chase, MD 20185; and §Department of Ophthalmology, Massachusetts Eye and Ear Infirmary, Boston, MA 02114

Communicated by Phillip A. Sharp, Massachusetts Institute of Technology, Cambridge, MA, January 3, 2007 (received for review October 5, 2006)

Tissue fusion, the morphogenic process by which epithelial sheets are drawn together and sealed, has been extensively studied in *Drosophila*. However, there are unique features of mammalian tissue fusion that remain poorly understood. Notably, detachment and apoptosis occur at the leading front in mammals but not in invertebrates. We found that in the mouse embryo, expression of the *Nf2* tumor suppressor, merlin, is dynamically regulated during tissue fusion: *Nf2* expression is low at the leading front before fusion and high across the fused tissue bridge. Mosaic *Nf2* mutants exhibit a global defect in tissue fusion characterized by ectopic detachment and increased detachment-induced apoptosis (anoikis). By contrast with core components of the junctional complex, we find that merlin is required specifically for the assembly but not the maintenance of the junctional complex. Our work reveals that regulation of *Nf2* expression is a previously unrecognized means of controlling adhesion at the leading front, thereby ensuring successful tissue fusion.

neurofibromatosis type 2

Tissue fusion is the morphogenic process by which epithelial sheets are drawn together and sealed to form a continuous layer. Failure of tissue fusion is common during human embryogenesis and the consequences can be severe. For example, neural tube defects (NTDs) that disrupt either the closing of the cranial neural tube (prospective brain) or spinal neural tube (prospective spinal cord) affect 3,000 pregnancies per year in the United States and cause life-threatening neurologic deficits (1).

Tissue fusion has been extensively studied in the *Drosophila* embryo, where the last major morphogenic event is a tissue fusion event termed dorsal closure. Although many molecular mechanisms important for tissue fusion appear highly conserved between flies and mammals (2), there are important differences. First, the *Drosophila* dorsal hole is significantly smaller than the mammalian holes that need to be sealed. By contrast with *Drosophila* where the dorsal hole can be covered by migration and dorsoventral elongation of existing epidermal cells, cell proliferation is essential for mammalian tissue fusion (3). Second, mammalian tissue fusion requires apoptosis. In the case of neural tube closure, apoptotic cells are located at the tips of the unfused neural folds, in the adjacent dorsolateral neural plate, and in the dorsal midline immediately after fusion has taken place. Preventing apoptosis with peptide caspase inhibitors blocks neural tube closure in explanted chick embryos, demonstrating that apoptosis is not simply an unavoidable by-product of the fusion process but probably plays an essential physiological role (4). Consistent with this, multiple mouse mutants with decreased levels of apoptosis in the neuroepithelium exhibit NTDs (3). Third, in mammalian but not invertebrate tissue fusion, there is loosening of cell–cell adhesion at the leading front (LF), accompanied by the complete detachment of many cells (5, 6). Once a mammalian hole is closed, strong cell–cell contacts must be established to stabilize the newly formed tissue bridge. Thus, cell–cell adhesion is likely to be regulated in a highly dynamic manner during mammalian tissue fusion.

Neurofibromatosis type 2 (NF2) is an autosomal dominant disorder in which patients develop neoplasms of the central and peripheral nervous systems. The *Nf2* gene product merlin is closely related to the ezrin-radixin-moesin proteins, which link plasma membrane proteins to the actin cytoskeleton (7, 8). Merlin may have multiple molecular functions including: 1) down-regulation of Rac-dependent signaling by inhibition of p21-activated kinase 1 (PAK1) or suppression of recruitment of Rac to the membrane (9, 10), 2) regulation of the actin cytoskeleton via a direct interaction between an N-terminal domain in merlin and actin filaments or indirectly through actin-associated proteins (11), and 3) regulation of receptor endocytosis and signaling (12, 13).

In vitro studies of primary cells by Lallemand and coworkers indicate that merlin may play an additional role in stabilizing adherens junctions (AJs) at sites of cell–cell contact (14). Merlin localizes to AJs, and loss of *Nf2* in keratinocytes prevents AJ formation. These initial findings raise a number of interesting questions. Is merlin required to stabilize the junctional complex [tight junctions (TJs) and AJs] *in vivo*? Is merlin required for the assembly and/or maintenance of the junctional complex? And, is merlin's affect on junctional complex stability related to its other molecular functions?

In this study, we find that regulation of *Nf2* tumor suppressor, merlin, is a novel means of controlling adhesion at the LF during tissue fusion. We provide *in vivo* evidence that merlin, unlike core components of the junctional complex, is required specifically for the assembly but not the maintenance of the junctional complex (TJs and AJs). This work provides a framework for understanding the unique aspects of mammalian tissue fusion and the role of merlin in development and cancer.

DEVELOPMENTAL BIOLOGY

Results

Dynamic Regulation of *Nf2* Expression at the LF During Tissue Fusion. *Nf2* is expressed widely during embryogenesis and in early postnatal life but becomes more restricted in the adult (15), suggesting that merlin may serve a particularly important func-

Author contributions: M.E.M., G.M.K., and T.J. designed research; M.E.M., G.M.K., K.L.S., D.C., N.A.M., J.H., and M.M. performed research; M.E.M., G.M.K., K.L.S., D.C., and N.A.M. contributed new reagents/analytic tools; M.E.M., G.M.K., K.L.S., and T.J. analyzed data; and M.E.M., G.M.K., and T.J. wrote the paper.

The authors declare no conflict of interest.

Freely available online through the PNAS open access option.

Abbreviations: LF, leading front; NTD, neural tube defect; VZ, ventricular zone; NE, neuroepithelial; ALJC, apico-lateral junctional complex; TJ, tight junction; AJ, adherens junction; tEM, transmission electron microscopy; E*n*, embryonic day *n*.

¶To whom correspondence should be addressed at: Massachusetts Institute of Technology, Center for Cancer Research, 40 Ames Street, E17-517, Cambridge, MA 02130. E-mail: tjacks@mit.edu.

This article contains supporting information online at www.pnas.org/cgi/content/full/0700044104/DC1.

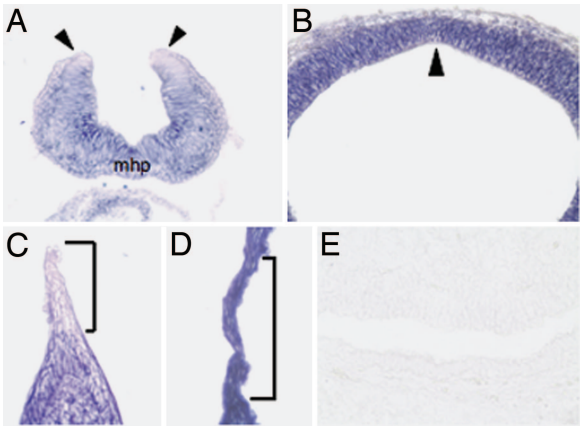

Fig. 1. Dynamic regulation of *Nf2* expression at the LF during tissue fusion. *In situ* hybridization of frozen sections using an antisense probe that recognizes the *Nf2* mRNA shows decreased *Nf2* expression in the dorsal NE cells at the tips of the forebrain neural folds at E9.25 (*A*, arrowheads) and in the peridermal and epidermal cells at the LF of the developing eyelids at E15.5 (*C*, bracket). After completion of neural tube closure (forebrain vesicle, E10.5) and eyelid fusion (E15.5), the NE cells (*B*) and epidermal cells (*D*) that form the respective tissue bridges show strong *Nf2* expression. The arrowhead in *B* marks the dorsal midline where the neural folds have fused. Bracket in *D* demarcates the junctional zone where eyelid fusion occurred. A control sense probe shows no staining of the VZ (E15.5) (*E*). mhp, median hinge point.

tion during development. To characterize the expression pattern of *Nf2* in greater detail, we performed *in situ* hybridization with an antisense digoxigenin riboprobe generated against the C-terminal half of *Nf2*. We analyzed mouse embryos at various stages of gestation from embryonic day 8.5 to 18.5 (E8.5–18.5). We found that *Nf2* levels were decreased in the dorsal neuroepithelial (NE) cells at the tips of the neural folds at E9.25 (Fig. 1*A*) and in the peridermal and epidermal cells at the LF of the developing eyelids at E15.5 (Fig. 1*C*). After completion of neural tube closure and eyelid fusion, the NE cells and epidermal cells that formed the respective tissue bridges showed strong *Nf2* expression (Fig. 1 *B* and *D*). *Nf2* expression remained strong in the ventricular/subventricular zone and developing cortex through E18.5 [supporting information (SI) Fig. 4 *A–C*]. Recently, Akhmametyeva and coworkers generated transgenic mice carrying a 2.4-kb *NF2* promoter driving β-gal and observed a transient decrease in β-gal staining at the tips of the neural folds before fusion (16). Our *in situ* hybridization data validates the use of these transgenic mice as surrogates for endogenous *Nf2* expression.

Detachment and apoptosis occurred at the exact location where *Nf2* levels were decreased (SI Figs. 4 *D–F* and 9*D*), suggesting that changes in *Nf2* expression may impact on the timing and location of detachment and apoptosis during tissue fusion.

Deletion of Nf2 in the Embryo by Asynchronous *NesCre1^p*-Mediated Recombination. $Nf2^{-/-}$ mouse embryos die early in gestation (E6.5–7) due to an extraembryonic defect (17), thus the consequences of *Nf2* loss in the embryo proper remain largely unknown. To test whether merlin was required for tissue fusion, specifically neurulation, we combined a conditional loss-of-function allele of *Nf2* ($Nf2^{flox2}$) with a Cre recombinase transgene expressed from the nestin promoter (*NesCre1*) (18, 19). We and other groups have observed different levels of Cre-mediated recombination from the *NesCre1* transgene depending on whether the transgene is inherited from the father or mother, presumably due to imprinting effects (20) (SI Fig. 5). The experiments described in this manuscript were performed by using $Nf2^{flox2}$ embryos with paternally inherited *NesCre1* (designated *NesCre1^p*); we refer to these embryos below as "*NesCre1^p Nf2* mosaics."

The *NesCre1^p* transgene provided an ideal system in which to study neurulation, as *NesCre1^p*-mediated recombination could be detected in scattered NE cells at E8.5, before neural tube closure (SI Fig. 6*A*). By late gestation (E18.5), virtually all of the cells in the brains of *NesCre1^p*-positive mice had undergone recombination (SI Fig. 6*B*). Near complete *NesCre1^p*-mediated recombination in the brains of late gestation *NesCre1^p Nf2* mosaics was confirmed by PCR (SI Fig. 6*C*) and Western blotting for merlin (SI Fig. 6*D*). This data demonstrated that *NesCre1^p*-mediated recombination was asynchronous, with a subset of NE cells losing *Nf2* expression early in midgestation and the remainder of NE cells and their progeny losing *Nf2* expression in mid-to-late gestation. The asynchrony of *NesCre1^p* -mediated recombination provided us with the unique opportunity to compare the role of merlin in the assembly versus the maintenance of the junctional complexes within the neuroepithelium.

Global Tissue Fusion Defect in *NesCre1^p Nf2* Mosaics. Although the vast majority of the *NesCre1^p Nf2* mosaics survived until the time of birth (SI Table 1), these embryos exhibited a striking defect in tissue fusion. We observed a spectrum of NTDs, including encephalocele, exencephaly and rarely completely open neural tubes (Fig. 2 *A–C*). Intriguingly, we recovered 8.6 times more embryos with exencephaly at E18.5 (17 exencephalic embryos/142 total embryos including all genotypes) than at E9.5 (2 exencephalic embryos/146 total embryos including all genotypes), suggesting that the major mechanism of exencephaly was neural tube reopening. The cause of reopening may be an accumulation of *Nf2*-deficient cells defective in cell–cell adhesion and apoptosis (see below).

In addition to NTDs, we observed three tissue fusion defects in the eye (retinal coloboma, lens herniation, and open-eyelids-at-birth) (Fig. 2 *D–F*), cleft palate (Fig. 2*G*), omphalocele (Fig. 2*H*), and cardiac ventricular septal defects (Fig. 2*I*). All tissue fusion defects had incomplete penetrance (SI Table 2). Defects in chorioallantoic fusion were not detected. In the mouse, this tissue fusion event occurs at E8.5, a time when *NesCre1^p*-mediated recombination is only present in scattered cells in the embryo. A variety of other defects affecting tissue organization and differentiation were also identified in the *NesCre1^p Nf2* mosaics (SI Figs. 7 and 8).

Merlin Prevents Ectopic Detachment by Promoting the Formation of Apico-Lateral Junctional Complexes. To understand why tissue fusion was failing in the *NesCre1^p Nf2* mosaics, we studied the NTDs in detail. We compared *NesCre1^p Nf2* mosaics to developmentally matched wild-type embryos (Fig. 2 *J* and *L*), as morphogenetic progression causes marked changes in the structure of the neural tube and frequency of apoptosis, making age-matched controls uninformative. Histologic examination of transverse sections through the brains of E9.5 *NesCre1^p Nf2* mosaics revealed that NE cells were detaching from the apical surface. In mutants with closed neural tubes, the detached NE cells accumulated within the ventricular space (Fig. 2*K*). Along the dorsal neural tube where tissue fusion occurred, the NE cells and epidermal ectoderm appeared disorganized, likely predisposing the embryo to neural tube reopening. Severely affected mutants showed widespread detachment of NE cells and cells from the epidermal ectoderm (Fig. 2*M*). In these mutants, there were likely too few cells remaining for neurulation to proceed. Histologically, the majority of detaching epithelial cells appeared viable: completely detached cells undergoing mitosis were identified (Fig. 2*K*, upper inset).

Ultrastructural examination of the neuroepithelium revealed the cause of ectopic detachment. By transmission electron

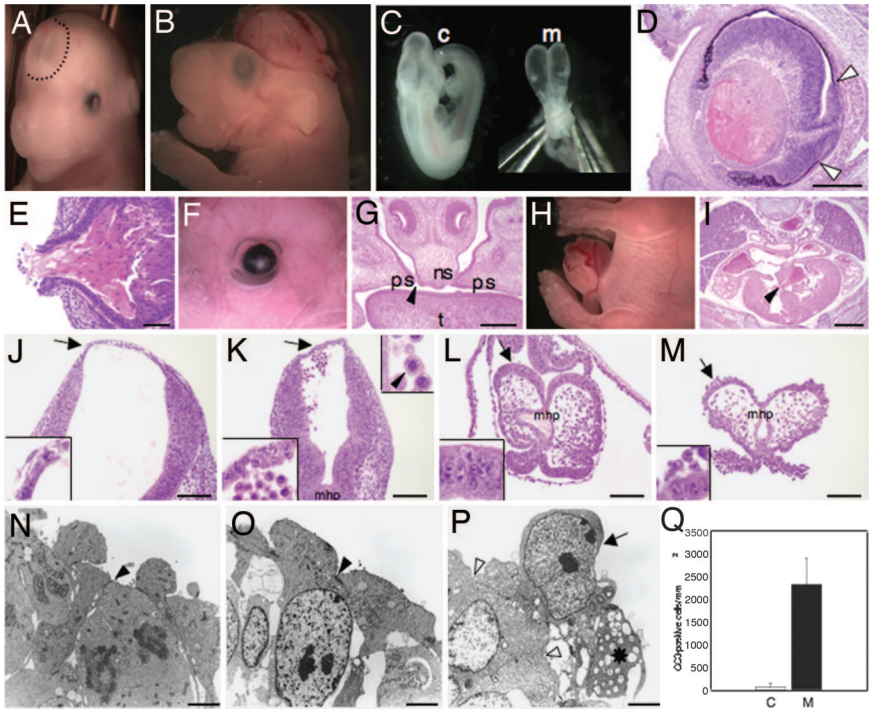

Fig. 2. Global tissue fusion defect in *NesCre1^{p} Nf2* mosaics. A spectrum of NTDs is observed in *NesCre1^{p} Nf2* mosaics. Examples of an encephalocele (dotted line) in an E15.5 mutant (*A*), exencephaly in an E18.5 mutant (*B*), and a completely open neural tube in an E9.5 mutant (m) (*C*) are shown. The E9.5 mutant with a completely open neural tube is significantly smaller than a wild-type E9.5 control (c). Other tissue fusion defects include the following: retinal coloboma (*D*) (note the discontinuity of the retinal pigment epithelium between the open arrowheads and associated retinal dysplasia), lens herniation (*E*), open-eyes-at-birth (*F*), cleft palate (*G*, closed arrowhead), omphalocele (*H*), and cardiac ventricular septal defect (*I*, closed arrowhead). Transverse sections through the brains of E9.5 (*J*) and E8.25 (*L*) control embryos are compared with transverse sections at the same anatomic level through the brains of a mildly affected E9.5 mutant embryo (*K*) and a severely affected E9.5 mutant embryo (*M*). Arrows in *J–M* indicate the regions that are shown at higher magnification in the lower insets. In the mildly affected mutant with a closed neural tube, the detached cells accumulate within the ventricular space. In the severely affected mutant, the detached cells are released into the amniotic fluid. The majority of the detached cells appear viable, and an example of a completely detached cell undergoing mitosis is shown (*K*, upper inset, closed arrowhead). The NE cells and epidermal cells that comprise the tissue bridge in the mildly affected mutant (*K*, lower inset) appear disorganized. tEM of the NE cells along the wall of the neural fold in an E8.5 control embryo (*N*) and an E9.5 severely affected mutant (*O* and *P*) reveals focally absent ALJCs in the mutant (*P*, open arrowheads). In the control embryo and other regions of the neuroepithelium in the mutant, regularly spaced ALJCs are identified (*N* and *O*, closed arrowheads). A viable-appearing NE cell that is detaching from the apical surface (*P*, arrow) is seen in the region where junctions are absent. An adjacent cell that has detached is undergoing apoptosis (*P*, asterisk). Immunohistochemistry for the apoptotic marker CC3 demonstrated a marked increase in apoptosis in the mutant neuroepithelium (*Q*). ps, palatal shelf; ns, nasal septum; t, tongue; C, control; M, mutant; mhp, median hinge point. [Scale bars: 250 μm (*D*), 100 μm (*E*), 1,000 μm (*G* and *I*), 200 μm (*J–M*), and 3 μm (*N–P*).]

microscopy (tEM), we found areas of neuroepithelium in *NesCre1^{p} Nf2* mosaics in which the apico-lateral junctional complexes (ALJCs) were absent (Fig. 2*P*). Some NE cells in these areas were detached from the apical surface. Whereas some detached NE cells appeared viable, others showed signs of apoptosis, such as numerous cytoplasmic vacuoles. The remainder of the neuroepithelium in the *NesCre1^{p} Nf2* mosaics had normally distributed ALJCs (Fig. 2*O*), consistent with the mosaic pattern of *NesCre1^{p}* activity at this stage in development. Thus, merlin is required *in vivo* for the assembly of ALJCs in the developing nervous system.

We investigated the relationship among *Nf2* expression, detachment, and apoptosis using immunohistochemistry against the apoptotic marker, cleaved caspase-3 (CC3). As reported (21), apoptotic cells in the neuroepithelium of E8.5 controls were predominantly localized to the tips of the neural folds (SI Fig. 9*D*). Within severely affected E9.5 mutants, the level of apoptosis was increased 38.7-fold compared with the developmentally matched E8.5 controls (*t* test $P = 0.0005$) (Fig. 2*Q*). Furthermore, apoptotic cells were not restricted to the tips of the neural folds but were found throughout the neural plate (SI Fig. 9*E*). 91.2% of NE cells that had detached in the *NesCre1^{p} Nf2* mosaic embryos were negative for CC3, consistent with detachment preceding and triggering apoptosis, a phenomenon known as anoikis. Immunohistochemistry for the proliferation marker Ki-67 revealed a similar, very high rate of proliferation within the neuroepithelium of E8.5 controls and severely affected E9.5 mutants (SI Fig. 9 *A–C*). Together, these findings suggest that deletion of *Nf2* inhibits the formation of ALJCs, leading to ectopic detachment and anoikis of NE cells. Furthermore, reduced levels of *Nf2* at the LF may promote detachment and apoptosis at this site during the normal process of tissue fusion.

Analysis of Merlin Using a Functional Cell–Cell Adhesion Assay. We demonstrated *in vivo* that merlin is required for the assembly of ALJCs in the neuroepithelium. To quantify this effect, we used a hanging drop assay that measures the ability of single cells to form cell aggregates and the resistance of these aggregates to a shearing force. MDCK epithelial cells were selected for this experiment because the majority of tissue fusion events involve epithelial cells, and the use of these cells in the hanging drop assay is well established. MDCK cells were transfected with either an empty vector expressing GFP (control) or a vector coexpressing a dominant-negative form of *Nf2* and GFP. Pure populations of GFP-positive cells were isolated by FACS analysis. Overexpression of dominant-negative merlin was confirmed by Western blotting (SI Fig. 10*A*).

At the beginning of the experiment, all of the cells in the

hanging drops were present as single cells (SI Fig. 10 *B–D*). In the control (SI Fig. 10 *B* and *D*), the number of cells in large clusters (>25 cells) increased to 31% at 2 h, and to 64% at 4 h. Resistance to trituration increased from 0% of cells remaining in large clusters at 2 h, to 42% of cells at 4 h. Cells expressing dominant-negative *Nf2* formed large clusters of >25 cells more slowly, with only 11% of cells in large clusters at 2 h (SI Fig. 10 *C* and *D*). Furthermore, the cells expressing dominant-negative *Nf2* were more sensitive to trituration. At 4 h, 66% of these cells were present in large clusters; after trituration only 23% remained in the large clusters. Thus, dominant-negative merlin decreased both the rate and strength of adhesion. Consistent with this result, immunocytochemistry of MDCK cells expressing dominant-negative merlin showed decreased AJ formation (SI Fig. 11), whereas the distribution of focal adhesions appeared unaffected (SI Fig. 12). The hanging drop assay is the first direct functional test of merlin's role in adhesion.

Merlin Is Required for the Assembly but Not Maintenance of Apico-Lateral Junctional Complexes. After neural tube closure, the NE cells and NE-derived radial glia that line the ventricles [ventricular zone (VZ) cells] do not assemble *de novo* ALJCs (22, 23). Instead, inheritance of existing ALJCs is determined by the orientation of cleavage during cell division. Electron and confocal microscopy show that a horizontal cleavage produces an apical daughter cell that inherits the entire ALJC and a basal daughter that is specified to become a migratory neuron. By contrast, in a vertical division the cleavage furrow progresses from the basal toward the apical cell surface, where it bisects the existing ALJC between the two daughter cells. Even during mitosis when the VZ cells round up at the ventricular surface, the ALJCs are retained. Therefore, the neuroepithelium before and after neural tube closure offers a unique setting in which the requirement for merlin in ALJC assembly versus maintenance can be assessed *in vivo*.

In the subset of *NesCre1^{p} Nf2* mosaics in which the neural tube closed and remained closed, we examined the VZ in late gestation and found that it had a biphasic appearance. There were discrete clumps of disorganized, loosely attached VZ cells that protruded into the ventricular space, surrounded by well organized, pseudostratified VZ cells (Fig. 3*A*). tEM showed an absence of ALJCs within the disorganized clumps (Fig. 3*B*), and immunofluoresence for the TJ component, ZO-1, and the AJ components, N-cadherin and β-catenin, further confirmed the lack of ALJCs (Fig. 3 *D–F*). Although present, the apical band of actin was fragmented across the surface of the clumps (Fig. 3*G*).

Interestingly, tEM demonstrated the presence of ALJCs composed of distinct TJs and AJs within the well organized VZ (Fig. 3 *B* and *C*). By immunofluoresence, ZO-1, N-cadherin, β-catenin, and actin were properly localized (Fig. 3 *D–F*). In fact, TJs were more prominent in the mutant VZ than in the control, possibly reflecting a delay in differentiation (24). Thus, despite the fact that by late gestation there was very little if any merlin remaining in the brains of the *NesCre1^{p} Nf2* mosaics, the ALJCs in the well organized regions of the VZ were retained.

To verify that merlin was absent in the well organized regions of the VZ, we took three approaches. First, X-gal staining of *NesCre1^{p} Nf2* mosaics carrying the lox-STOP-lox *LacZ* reporter demonstrated blue staining in the disorganized clumps and in the well-organized VZ, indicating Cre-mediated recombination had occurred (SI Fig. 13*A*). Second, we performed laser capture microdissection followed by PCR on the well organized VZ and found complete recombination of the *Nf2^{2lox}* allele to the *Nf2^{1lox}* form (SI Fig. 13*B*). Third, immunohistochemistry with an anti-merlin antibody confirmed the absence of merlin in the mutant VZ (SI Fig. 13*D*).

This data in combination with the *NesCre1^{p}* reporter analysis showing asynchronous recombination indicates that NE cells

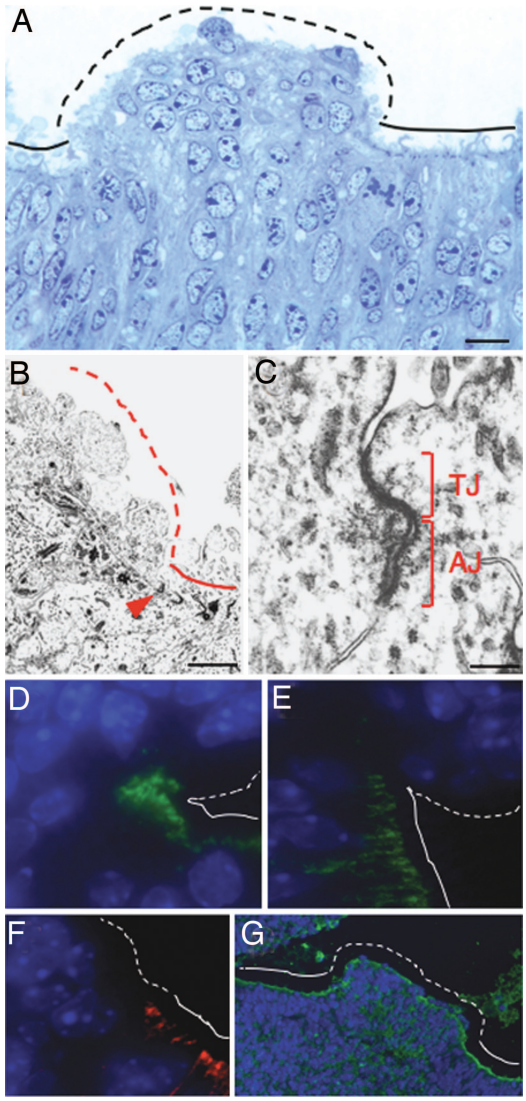

Fig. 3. Requirement for merlin in the assembly but not maintenance of ALJCs. A semithin section of the VZ at E18.5 shows a clump of disorganized, loosely attached VZ cells, surrounded by well organized VZ (*A*). tEM at such a border reveals that ALJCs are present in the well organized VZ but not within the disorganized clumps (closed red arrowhead marks an ALJC) (*B*). A higher magnification image demonstrates distinct TJs and AJs in the well organized VZ (*C*). The presence of TJs and AJs in the well organized VZ but not in the disorganized clumps is confirmed by immunofluorescence for the TJ-component ZO-1 (*D*) and the AJ-components, N-cadherin (*E*) and β-catenin (*F*). Immunofluoresence for β-actin shows that the apical bundle of actin filaments is present in the well organized VZ but is fragmented across a clump of disorganized VZ cells (*G*). Solid lines in *A* and *B* and *D–G* indicate the apical/ventricular side of VZ cells in well organized areas, and dashed lines indicate the apical/ventricular side of disorganized clumps of VZ cells. [Scale bars: 20 μm (*A*), 2.3 μm (*B*), and 0.3 μm (*C*).]

that lose *Nf2* early in gestation fail to assemble ALJCs and are prone to detaching, whereas NE cells and NE-derived radial glia that lose *Nf2* later in gestation are able to maintain existing ALJCs. This finding that merlin is required for the assembly but not the maintenance of ALJCs is completely unexpected based on the prior *in vitro* studies and contrasts sharply with the phenotype of mouse embryos in which core components of the junctional complex are deleted. Asynchronous deletion of β-catenin in the developing forebrain (between E8.75 and E10.5), for example, results in loss of the entire forebrain and

anterior facial structures, not exencephaly (25, 26). AJs are completely absent from the NE cells of these *FoxG1Cre;β-catenin*$^{fl/fl}$ embryos at E9.5, and there is massive detachment of NE cells into the ventricular space, consistent with a requirement for β-catenin in assembly and maintenance of the AJs.

Discussion

Successful morphogenesis in the mammalian embryo requires the completion of multiple tissue fusion events. In contrast to dorsal closure in *Drosophila*, mammalian tissue fusion is characterized by detachment and apoptosis at the LF. Little is known about the physiologic role of these processes and how they are controlled. In this report, we show that the expression of the *Nf2* tumor suppressor, merlin, is dynamically regulated during tissue fusion, with decreased levels at the LF before fusion and high levels across the fused tissue bridge.

The upstream pathways that regulate *Nf2* expression remain to be elucidated. Both BMP and Wnt/β-catenin signaling pathways are attractive candidates to regulate *Nf2* transcription, as mutations in either pathway can lead to NTDs in mice (27, 28). Several BMP ligands and targets of BMP signaling are expressed in dorsal neural tissue, where *Nf2* levels are transiently decreased. During brain development, Wnt/β-catenin signaling up-regulates expression of the *Sp5* gene, a member of the Sp1 transcription factor family that has the same DNA binding specificity as Sp1 but represses Sp1 target genes (29). Site-directed mutagenesis studies of the *NF2* promoter indicate that there is a GC-rich sequence (position −58 to −46) that can be bound by Sp1 (30), and possibly may be repressed by Sp5.

Merlin, in turn, regulates the assembly of ALJCs, acting as a developmental switch to loosen and tighten cell–cell adhesion. We provide evidence that loosening of cell–cell adhesion (detachment) may serve as a trigger of apoptosis at the LF, and propose that detachment-induced apoptosis (anoikis) may ensure that only those epithelial cells that form stable cell–cell contacts survive to contribute to the tissue bridge. As merlin has been previously shown to associate with β1-integrin complexes (31), it is also possible that loosening of cell-matrix interactions may contribute to detachment and anoikis.

We find that merlin is required *in vivo* for the assembly but not maintenance of ALJCs. The process of junctional complex assembly has been studied extensively in MDCK epithelial cells. In this model system, transinteractions between E-cadherin molecules initiate adhesion between adjacent cell membranes (32). This is followed by the formation of a primordial junction composed of AJ and TJ components, which matures into a distinct TJ and AJ. Remodeling of cortical actin and localized lamellipodial activity occur early in the process of initiating cell–cell contacts and correlate with the spatiotemporal regulation of Rac: Rac transiently concentrates at the newest sites of contact and decreases at older, stabilized sites (33). Thus, one model is that merlin might regulate junctional complex assembly by inhibiting Rac-dependent signaling. However, there was no increase in the Rac effector phospho-c-Jun either at the LF in normal embryos nor in mutant embryos (M.E.M. and T.J., data not shown), suggesting that decreased *Nf2* expression does not lead to a dramatic increase in Rac-dependent signaling in this developmental context. It is possible that merlin inhibits Rac in specific subcellular compartments, such as the site of cell–cell contact. Merlin may also regulate junctional complex assembly through regulation of the actin cytoskeleton or receptor density at the cell surface, as both actin and signaling receptors are intimately associated with the ALJC (34, 35). As merlin is dispensable for the maintenance of the ALJC, it is unlikely that merlin serves as a core structural component.

Our finding that merlin is required for the assembly but not maintenance of ALJCs has important implications for the role of *NF2* loss in tumorigenesis. If *NF2* loss occurs in a nondividing cell with mature junctional complexes, there may be no adverse consequences. However, if *NF2* loss occurs in a dividing cell or a nondividing cell that at a later point in time reenters the cell cycle and needs to assemble junctional complexes *de novo* (e.g., during tissue repair), then tumorigenesis may be initiated: cells that cannot form ALJCs and establish apicobasal polarity will be unable to form a well-organized tissue and will be resistant to contact-dependent growth arrest. Notably, it has long been recognized that the risk for developing a meningioma, a tumor that frequently harbors *NF2* mutations, is significantly increased in patients with a history of head trauma (36, 37). Thus, the elucidation of the consequences of *Nf2* deficiency in the developing embryo may provide a framework to understand how germline and sporadic mutations of this tumor suppressor contribute to tumor formation.

Materials and Methods

SI Methods provide further details.

RNA *In Situ* Hybridization. We used a modification of the methods described by Wilkinson and Nieto to perform *in situ* hybridization on 15-μm frozen sections of E8.5-E18.5 embryos (38). The primers 5′-TTACTATTAAACCACTGG-3′ and 5′-CGCTTCATGTCCGTATCC-3′ were used to PCR amplify an 836-bp fragment from the C-terminal half of the *Nf2* cDNA. This fragment was cloned into the pCR-Blunt II-TOPO vector (Invitrogen, Carlsbad, CA), creating pMB84. By using primers to the SP6 promoter and the T7 promoter, linear DNA fragments containing the 836-bp *Nf2* fragment were generated by PCR amplification. An antisense digoxigenin riboprobe for *Nf2* was generated by incubating the linear DNA fragments with SP6 RNA polymerase, and a sense digoxigenin riboprobe for *Nf2* was generated by incubating the linear DNA fragments with T7 RNA polymerase.

tEM. Whole E8.5 and E9.5 embryos or eyes and surrounding soft tissue from E15.5 embryos were placed into fixative consisting of 2.5% glutaraldehyde and 2% formaldehyde in 0.1 M cacodylate buffer with 0.08 M $CaCl_2$ for 24 h at 4°C. Specimens were processed and viewed as described (39).

Mice and Generation of Embryos. *NesCre1* transgenic mice were obtained from Andreas Trumpp (Swiss Institute for Experimental Cancer Research, Lausanne, Switzerland) and *Nf2*$^{flox2/flox2}$ mice were obtained from Marco Giovannini (Foundation Jean Dausset-Centre d'Etude du Polymorphisme Humain, Paris, France). *NesCre1* mice were crossed to *Nf2*$^{flox2/flox2}$ mice. Male offspring expressing Cre were crossed to *Nf2*$^{flox2/flox2}$ females. *NesCre1* mice were separately crossed to lox-STOP-lox LacZ reporter mice Gt(ROSA)26Sor^{tm1Sor} (Jackson Laboratories, Bar Harbor, ME) to generate offspring with paternally or maternally inherited Cre. *NesCre1;Nf2*$^{flox2/+}$ male mice were also crossed to *Nf2*$^{flox2/flox2}$; Gt(ROSA)26Sor^{tm1Sor} female mice to generate mutant embryos containing the lox-STOP-lox LacZ reporter. Details of PCR genotyping reactions are available upon request. The morning of plug detection was taken as E0.5, and embryos were collected from mid-gestation to birth. Embryos were dissected from the mother, either the yolk sac or the tail was collected for genotyping, and embryos were fixed overnight in Bouin's fixative, 10% neutral buffered formalin (NBF), or 4% paraformaldehyde (PFA) in PBS. Embryos were processed and embedded in paraffin, and 4-μm sections were cut. Research was conducted in compliance with the Animal Welfare Act Regulations and other federal statutes relating to animals and experiments involving animals and adheres to the principles set forth in the

Guide for Care and Use of Laboratory Animals, National Research Council, 1996.

Immunohistochemistry and Immunofluorescence. Whole E8.5 and E9.5 embryos or brains from E15.5 and E18.5 embryos were fixed in 10% NBF for 1 h or 24 h, respectively. For detecting merlin by immunohistochemistry, brains from E18.5 embryos were snap-frozen. Seven-micrometer sections were cut and fixed in acetone at 4°C for 10 min. We used a modification of the methods described by M.E.M and J.T. to perform immunohistochemistry and immunofluoresence (40). The following antibodies were used: Ki-67 (Novocastra, Newcastle, United Kingdom; 1/200), CC3 (Cell Signaling, Beverly, MA; 1/100), merlin (Cell Signaling; #9168, 1/100), ZO-1 (Zymed Laboratories, South San Francisco, CA; 1/50), N-cadherin (BD Transduction Laboratories, San Jose, CA; 1/100), β-catenin (Cell Signaling; 1/100), and β-actin (Sigma, St. Louis, MO; 1/50). Ki-67 and CC3-positive cells and tissue areas were determined by using Bioquant Image Analysis software in manual measurement mode.

We thank A. Charest, C. Kim, K. Ligon, D. MacPherson, D. Pellman, and A. Shaw for helpful discussions and critical review of the manuscript. We thank N. Young, D. Yuk, N. Watson, and B. Margolis and members of his laboratory for technical assistance. We are grateful to M. Giovannini for providing the *Nf2* conditional mice and A. Trumpp for providing the *NesCre1* transgenic mice. This work was sponsored by the Department of the Army (award no. DAMD17-02-1-0638 and subsequently W81-XWH-05-1-265). T.J. is an Investigator of the Howard Hughes Medical Institute. M.E.M. was supported by a Burroughs Wellcome Fund Career Award in the Biomedical Sciences.

1. Centers for Disease Control (2004) *Morb Mortal Wkly Rep* 53:362–365.
2. Martin P, Wood W (2002) *Curr Opin Cell Biol* 14:569–574.
3. Copp AJ, Greene ND, Murdoch JN (2003) *Nat Rev Genet* 4:784–793.
4. Weil M, Jacobson MD, Raff MC (1997) *Curr Biol* 7:281–284.
5. Findlater GS, McDougall RD, Kaufman MH (1993) *J Anat* 183(Pt 1):121–129.
6. Martinez-Alvarez C, Tudela C, Perez-Miguelsanz J, O'Kane S, Puerta J, Ferguson MW (2000) *Dev Biol* 220:343–357.
7. Rouleau GA, Merel P, Lutchman M, Sanson M, Zucman J, Marineau C, Hoang-Xuan K, Demczuk S, Desmaze C, Plougastel B, *et al.* (1993) *Nature* 363:515–521.
8. Trofatter JA, MacCollin MM, Rutter JL, Murrell JR, Duyao MP, Parry DM, Eldridge R, Kley N, Menon AG, Pulaski K, *et al.* (1993) *Cell* 72:791–800.
9. Kissil JL, Wilker EW, Johnson KC, Eckman MS, Yaffe MB, Jacks T (2003) *Mol Cell* 12:841–849.
10. Okada T, Lopez-Lago M, Giancotti FG (2005) *J Cell Biol* 171:361–371.
11. McClatchey AI, Giovannini M (2005) *Genes Dev* 19:2265–2277.
12. Hamaratoglu F, Willecke M, Kango-Singh M, Nolo R, Hyun E, Tao C, Jafar-Nejad H, Halder G (2006) *Nat Cell Biol* 8:27–36.
13. Maitra S, Kulilauskas RM, Gavilan H, Fehon RG (2006) *Curr Biol* 16:702–709.
14. Lallemand D, Curto M, Saotome I, Giovannini M, McClatchey AI (2003) *Genes Dev* 17:1090–1100.
15. Bianchi AB, Hara T, Ramesh V, Gao J, Klein-Szanto AJ, Morin F, Menon AG, Trofatter JA, Gusella JF, Seizinger BR, *et al.* (1994) *Nat Genet* 6:185–192.
16. Akhmametyeva EM, Mihaylova MM, Luo H, Kharzai S, Welling DB, Chang LS (2006) *Dev Dyn* 235:2771–2785.
17. McClatchey AI, Saotome I, Ramesh V, Gusella JF, Jacks T (1997) *Genes Dev* 11:1253–1265.
18. Giovannini M, Robanus-Maandag E, van der Valk M, Niwa-Kawakita M, Abramowski V, Goutebroze L, Woodruff JM, Berns A, Thomas G (2000) *Genes Dev* 14:1617–1630.
19. Trumpp A, Depew MJ, Rubenstein JL, Bishop JM, Martin GR (1999) *Genes Dev* 13:3136–3148.
20. Fan G, Beard C, Chen RZ, Csankovszki G, Sun Y, Siniaia M, Biniszkiewicz D, Bates B, Lee PP, Kuhn R, *et al.* (2001) *J Neurosci* 21:788–797.
21. Geelen JA, Langman J (1977) *Anat Rec* 189:625–640.
22. Hinds JW, Ruffett TL (1971) *Z Zellforsch* 115:226–264.
23. Chenn A, Zhang YA, Chang BT, McConnell SK (1998) *Mol Cell Neurosci* 11:183–193.
24. Aaku-Saraste E, Hellwig A, Huttner WB (1996) *Dev Biol* 180:664–679.
25. Hebert JM, McConnell SK (2000) *Dev Biol* 222:296–306.
26. Junghans D, Hack I, Frotscher M, Taylor V, Kemler R (2005) *Dev Dyn* 233:528–539.
27. Stottmann RW, Berrong M, Matta K, Choi M, Klingensmith J (2006) *Dev Biol* 295:647–663.
28. Carter M, Chen X, Slowinska B, Minnerath S, Glickstein S, Shi L, Campagne F, Weinstein H, Ross ME (2005) *Proc Natl Acad Sci USA* 102:12843–12848.
29. Fujimura N, Vacik T, Machon O, Vlcek C, Scalabrin S, Speth M, Diep D, Krauss S, Kozmik Z (2007) *J Biol Chem* 282:1225–1237.
30. Chang L-S, Akhmametyeva EM, Wu Y, Zhu L, Welling DB (2002) *Genomics* 79:63–76.
31. Fernandez-Valle C, Tang Y, Ricard J, Rodenas-Ruano A, Taylor A, Hackler E, Biggerstaff J, Iacovelli J (2002) *Nat Genet* 31:354–362.
32. Matter K, Balda MS (2003) *Nat Rev Mol Cell Biol* 4:225–236.
33. Ehrlich JS, Hansen MD, Nelson WJ (2002) *Dev Cell* 3:259–270.
34. Kobielak A, Pasiolli A, Fuchs E (2003) *Nat Cell Biol* 6:21–30.
35. Carmeliet P, Lampugnani MG, Moons L, Breviaro F, Compernolle V, Bono F, Balconi G, Spagnuolo R, Oostuyse B, Dewerchin M, *et al.* (1999) *Cell* 98:147–157.
36. Cushing H (1938) in *Meningiomas: Their Classification, Regional Behavior, Life History, and Surgical End Results* (Thomas, Baltimore), p 485.
37. Phillips LE, Koepsell TD, van Belle G, Kukull WA, Gehrels JA, Longstreth WT, Jr (2002) *Neurology* 58:1849–1852.
38. Wilkinson DG, Nieto MA (1993) *Methods Enzymol* 225:361–373.
39. Renno RZ, Terada Y, Haddadin MJ, Michaud NA, Gragoudas ES, Miller JW (2004) *Arch Ophthalmol* 122:1002–1011.
40. McLaughlin ME, Jacks T (2003) *Cancer Res* 63:752–755.